

A symmetry-breaking mechanism for the Z4 general-covariant evolution system

C. Bona, T. Ledvinka, C. Palenzuela and M. Žáček

Departament de Física, Universitat de les Illes Balears,
Ctra de Valldemossa km 7.5, 07071 Palma de Mallorca, Spain

The general-covariant Z4 formalism is further analyzed. The gauge conditions are generalized with a view to Numerical Relativity applications and the conditions for obtaining strongly hyperbolic evolution systems are given both at the first and the second order levels. A symmetry-breaking mechanism is proposed that allows one, when applied in a partial way, to recover previously proposed strongly hyperbolic formalisms, like the BSSN and the Bona-Massó ones. When applied in its full form, the symmetry breaking mechanism allows one to recover the full five-parameter family of first order KST systems. Numerical codes based in the proposed formalisms are tested. A robust stability test is provided by evolving random noise data around Minkowski space-time. A strong field test is provided by the collapse of a periodic background of plane gravitational waves, as described by the Gowdy metric.

PACS numbers:

I. INTRODUCTION

The waveform emitted in the inspiral and merger of a relativistic binary is a theoretical input crucial to the success of the laser interferometry gravitational laboratories [1, 2, 3, 4]. Although the regular orbiting phase can be treated with good accuracy by well-known analytical perturbation methods, the later phases belong clearly to the strong field regime of either a black hole or a neutron star collision, so that a computational approach is mandatory. This kind of computational effort has been the objective of the Binary Black Hole (BBH) Grand Challenge [5] and other world wide collaborations. The resulting numerical codes are based on the so called ADM formalism [6] for the Einstein field equations, where only a subset of the equations are actually used for evolution whereas the remaining ones are considered as constraints to be imposed on the initial data only (free evolution approach [7]).

It is clear that, by taking the constraints out of the evolution system, one is extending the solution space. This extension is the crucial step that opened the way to new hyperbolic formalisms after the seminal work of Y. Choquet-Bruhat and T. Ruggeri [8], using the constraints to modify the evolution system in many different ways [9, 10, 11, 12, 13, 14, 15, 16, 17, 18], even taking additional derivatives [8, 19, 20]. These formalisms can be interpreted as providing many non-equivalent ways of extending the solution space of Einstein's equations with at least one common feature: constraint equations are left out of the final evolution system.

This means that the resulting systems do have an extended solution space, which includes constraint-violating solutions in addition to the ones verifying the original Einstein's equations. As far as the constraints are first integrals of the extended evolution system, Einstein's solutions could be computed by solving the constraints equations only for the initial data (free evolution). But, unless some enforcing mechanism is used during the subsequent time evolution, numerical errors

will activate constraint-violating modes. Numerical simulations can deal with such modes, at least when the deviations from Einstein's solutions are moderate. But it happens that large deviations are usually associated with instabilities of constraint-violating modes, leading to code crashing.

In particular, numerical codes based on these new hyperbolic formalisms happen to be quite intolerant to violations of the Hamiltonian constraint in the initial data. This is a serious drawback if one is planning to use the results of the analytical approximation to the regular orbiting phase of a binary system as initial data for a numerical simulation of the final ringdown and merger. The numerical code will crash before any template for the gravitational wave emission could be extracted. This is because the analytical data are just a good approximation, so that the energy constraint does not hold exactly and the code is intolerant to that kind of "off-shell" initial data. Although there can be other options, we claim that a numerical code tolerant to constraint violation would be undoubtedly the best alternative.

There have been some attempts in that direction. In Ref. [21] the technique of Lagrange multipliers was used for including the constraints into the dynamical system. The extended system includes the Lagrange multipliers as additional dynamical fields (λ -system). A further step along that direction is given in Ref. [22], where the extended system is "adjusted" by further combining the evolution equations with the constraints, including then many extra arbitrary parameters. In both cases, the goal is to enforce the constraints in a dynamical way. One can monitor the errors by looking at the "subsidiary system", which can be derived from Bianchi identities and can be interpreted as the evolution system for constraint deviations. Parameters are adjusted in a way such that the characteristic speeds of the subsidiary system are either real and non-zero (so that the corresponding errors propagate away to the boundaries) or they have the right sign in the imaginary part to enforce damping (instead of exploding) the constraint deviations.

A simpler option (but not the only one, see for instance [24]) for including the constraints into the evolution system would be the general-covariant extension of the Einstein field equations proposed recently (Z4 system) [25]:

$$R_{\mu\nu} + \nabla_\mu Z_\nu + \nabla_\nu Z_\mu = 8\pi (T_{\mu\nu} - \frac{1}{2} T g_{\mu\nu}), \quad (1)$$

so that the full set of dynamical fields consists of the pair $\{g_{\mu\nu}, Z_\mu\}$. The solutions of the original field equations can then be recovered by imposing the algebraic constraint

$$Z_\mu = 0 \quad (2)$$

and the evolution of this constraint is subject to the linear homogeneous equation

$$\square Z_\mu + R_{\mu\nu} Z^\nu = 0, \quad (3)$$

which can be easily obtained from (1) allowing for the contracted Bianchi identities. Here again, by allowing for non-zero values of the extra four-vector Z_μ , one is extending the solution space. But now, as we will see in the following section, one is using all the field equations to evolve the pair $\{g_{\mu\nu}, Z_\mu\}$: no equation is taken out of the system and, as a result, general covariance is not broken. The initial metric $g_{\mu\nu}$ can be taken to be the one arising from analytical approximations and the initial four-vector Z_μ can be taken to vanish without any kind of inconsistency: one can even use the evolving values of Z_μ during the calculation as a good covariant indicator of the quality of the approximation.

Notice that (3) plays here the role of the subsidiary system. It is adjusted *ab initio*, without any parameter fine-tuning, because light speed is the only characteristic speed in (3). Constraint deviations, that is non-vanishing values of Z^μ will then propagate to the boundaries. The fact that our constraints (2) are algebraic will greatly simplify the task of providing outgoing boundary conditions that let the constraint deviations get out of the numerical grid [23]

Besides these considerations, there are other important theoretical issues that we will address in this work. The first one is a thorough analysis of the hyperbolicity of the evolution system. This is more or less straightforward for the first order version of the system, as discussed in Appendix B, but it is not so well known in the case of the second order version, discussed in Appendix A, where we have used the results of Kreiss and Ortiz [26] that recently shed light on this issue, which is crucial to discuss the well-posedness [27] of the evolution system (see also [28] for similar results for the BSSN system).

The second theoretical point that we want to stress here is that the Z4 system (1) is not just one more hyperbolic formalism to be added to the long list. As far as it is the only general covariant one, the question arises whether the existing non-covariant hyperbolic formalisms [9, 10, 11, 12, 13, 14, 15, 16, 17, 18] can be

recovered from (1) by some “symmetry breaking” mechanism. We have extended in this sense a previous work [29] where the deep relationship between the more widely used hyperbolic formalisms was pointed out. A partial symmetry breaking mechanism is presented in section II for recovering the second order systems [11, 12] and for the first order systems containing additional dynamical fields [9, 10] in section III. These sections are followed by another one containing numerical simulations that have been proposed recently [30] as standard test-beds for Numerical Relativity codes. A more general symmetry breaking mechanism is proposed in Appendix C to recover first order formalisms which do not contain additional dynamical fields [13, 14, 15, 16, 17, 18].

II. 3+1 EVOLUTION SYSTEMS

The general-covariant equations (1) can be written in the equivalent 3+1 form [25] (Z4 evolution system)

$$(\partial_t - \mathcal{L}_\beta) \gamma_{ij} = -2\alpha K_{ij} \quad (4)$$

$$\begin{aligned} (\partial_t - \mathcal{L}_\beta) K_{ij} = & -\nabla_i \alpha_j + \alpha [({}^3R_{ij} + \nabla_i Z_j + \nabla_j Z_i \\ & - 2K_{ij}^2 + (\text{tr} K - 2\Theta) K_{ij} \\ & - S_{ij} + \frac{1}{2} (\text{tr} S - \tau) \gamma_{ij}] \end{aligned} \quad (5)$$

$$\begin{aligned} (\partial_t - \mathcal{L}_\beta) \Theta = & \frac{\alpha}{2} [({}^3R + 2\nabla_k Z^k + (\text{tr} K - 2\Theta) \text{tr} K \\ & - \text{tr}(K^2) - 2Z^k \alpha_k / \alpha - 2\tau] \end{aligned} \quad (6)$$

$$\begin{aligned} (\partial_t - \mathcal{L}_\beta) Z_i = & \alpha [\nabla_j (K_i^j - \delta_i^j \text{tr} K) + \partial_i \Theta \\ & - 2K_i^j Z_j - \Theta \alpha_i / \alpha - S_i] \end{aligned} \quad (7)$$

where we have noted

$$\Theta \equiv \alpha Z^0, \quad \tau \equiv 8\pi \alpha^2 T^{00}, \quad S_i \equiv 8\pi \alpha T_i^0, \quad S_{ij} \equiv 8\pi T_{ij}. \quad (8)$$

In the form (4-7), it is evident that the Z4 evolution system consists only of evolution equations. The only constraints (2), that can be translated into:

$$\Theta = 0, \quad Z_i = 0, \quad (9)$$

are algebraic so that the full set of field equations (1) is actually used during evolution. This is in contrast with the ADM evolution system [6], which can be recovered from (4-7) by imposing (9). The first two equations (4,5) would transform into the well known ADM evolution system, whereas the last two equations (6,7) would transform into the standard energy and momentum constraints, namely

$$({}^3R + \text{tr}^2 K - \text{tr}(K^2)) = 2\tau \quad (10)$$

$$\nabla_j (K_i^j - \delta_i^j \text{tr} K) = S_i \quad (11)$$

In the “free evolution” ADM approach [7], both (10) and (11) were taken out of the evolution system: they

were imposed only on the initial data. This was consistent because (10,11) are first integrals of the ADM evolution system, but one can not avoid violations of (10,11) due to errors in numerical simulations or approximated initial data, as stated before. As a result, numerical simulations will deal as well with extended solutions. The main difference with the Z4 case, aside from covariance considerations, is that in the Z4 case the quantities Z_μ describing constraint deviations are included into the evolution system.

One can also ask in this context what happens if, instead of imposing of the full set (9), one imposes the single condition

$$\Theta = 0 \quad (12)$$

obtaining a system with only three supplementary dynamical variables Z_i of the kind determined in [29] (Z3 system): the one corresponding to the parameter choice

$$\mu = 2, \quad \nu = n = 0 \quad (13)$$

(we follow the notation of [29]).

One can easily understand two of the three conditions (13), namely

$$\mu = 2, \quad \nu = n, \quad (14)$$

because this amounts to the ‘physical speed’ requirement for the degrees of freedom not related to the gauge [29] and nothing else can arise from the general covariant equations (1) which are at our starting point. But values of the remaining parameter n other than zero would be very interesting. In particular, the choice

$$\mu = 2, \quad \nu = n = \frac{4}{3}. \quad (15)$$

would lead to the evolution system which is quasiequivalent (equivalent principal parts [29]) to the well known BSSN system [11, 12].

At this point, let us consider the following recombination of the dynamical fields

$$\tilde{K}_{ij} \equiv K_{ij} - \frac{n}{2} \Theta \gamma_{ij} \quad (16)$$

so that the Z4 system (4-7) can be written in a one-parameter family of equivalent forms just by replacing everywhere

$$K_{ij} \rightarrow \tilde{K}_{ij} + \frac{n}{2} \Theta \gamma_{ij}. \quad (17)$$

This kind of transformations leave invariant the solution space of the system (it is actually the same system expressed in a different set of independent fields). But if the suppression of the Θ field (12) is made after the replacement (17), one gets a one-parameter family of non-

equivalent systems (Z3 evolution systems), namely:

$$(\partial_t - \mathcal{L}_\beta) \gamma_{ij} = -2 \alpha K_{ij} \quad (18)$$

$$\begin{aligned} (\partial_t - \mathcal{L}_\beta) K_{ij} = & -\nabla_i \alpha_j + \alpha [{}^{(3)}R_{ij} + \nabla_i Z_j + \nabla_j Z_i \\ & - 2K_{ij}^2 + \text{tr} K K_{ij} - S_{ij} + \frac{1}{2}(\text{tr} S - \tau)\gamma_{ij}] \\ & - \frac{n}{4} \alpha [{}^{(3)}R + 2 \nabla \cdot Z + \text{tr}^2 K - \text{tr}(K^2) \\ & - 2(\alpha^{-1} \alpha_k) Z^k - 2\tau] \gamma_{ij} \quad (19) \\ (\partial_t - \mathcal{L}_\beta) Z_i = & \alpha [\nabla_j (K_i^j - \delta_i^j \text{tr} K) - 2K_i^j Z_j - S_i] \quad (20) \end{aligned}$$

where we have suppressed the tilde over K_{ij} , allowing for the vanishing of Θ .

The resulting system (18-20) is quasiequivalent (equivalent principal parts) to the ‘system A’ in ref. [29] verifying the ‘physical speed’ requirement (14). As we have already mentioned, it follows that the particular case

$$n = \frac{4}{3} \quad (21)$$

is quasiequivalent to the BSSN system [11, 12]. The system (18-21) can be decomposed into trace and trace-free parts

$$e^{4\phi} = \gamma^{1/3}, \quad \tilde{\gamma}_{ij} = e^{-4\phi} \gamma_{ij} \quad (22)$$

$$K = \gamma^{ij} K_{ij}, \quad \tilde{A}_{ij} = e^{-4\phi} (K_{ij} - \frac{1}{3} K \gamma_{ij}) \quad (23)$$

$$\tilde{\Gamma}_i = -\tilde{\gamma}_{ik} \tilde{\gamma}^{kj}_{,j} + 2 Z_i \quad (24)$$

to follow the correspondence with BSSN more closely. It must be pointed out, however, that one does not get in this way the original BSSN system: there is actually one difference in the lower order terms (only the principal parts are equivalent). The difference is in the term of the form

$$+\frac{n}{2} \alpha_k Z^k \gamma_{ij} \quad (25)$$

in the evolution equation (19), which is missing in the original BSSN system [12]. This lower order term is needed for consistency with the general covariant equations (1).

We have seen then how the widely used ADM and BSSN systems can be obtained from the more general Z4 formalism. The equivalence transformation (16) plays the crucial role because suppressing the Θ field (12) produces a sort of symmetry breaking: different values of the parameter n will lead to evolution systems that can no longer be transformed one into another once the set of dynamical fields is reduced by the disappearance of Θ . It can be regarded as a partial symmetry breaking mechanism for the original equations (4-6). The terms ‘‘partial’’

refers to the fact that only the quantity Θ is suppressed, while the Z_i are kept into the system (18-20). A complete symmetry breaking mechanism is discussed in Appendix C.

In section IV, we present the results of some test-bed simulations for the ADM and Z4 systems. We have considered for simplicity only vacuum space-times with the time coordinate conditions

$$(\partial_t - \mathcal{L}_\beta) \ln \alpha = -\alpha [f \text{tr} K - \lambda \Theta] \quad (26)$$

which are a further generalization of the one proposed in [25], where

$$f = 1, \quad \lambda = 2. \quad (27)$$

This two-parameter family of coordinate conditions is very interesting from the point of view of Numerical Relativity applications. But it is also interesting from the theoretical point of view, because it provides the opportunity to apply the recent results of Kreiss and Ortiz [26] on the hyperbolicity of the ADM system in a wider context. In Appendix A, we will use the same formulation (see ref. [27] for more details) to study the hyperbolicity of the Z4 system with the two-parameter family of dynamical gauge conditions (26).

III. FIRST ORDER SYSTEMS

A first order version of the Z4 evolution system (4-7) can be obtained in the standard way by considering the first space derivatives

$$A_k \equiv \alpha_k / \alpha, \quad D_{kij} \equiv \frac{1}{2} \partial_k \gamma_{ij} \quad (28)$$

as independent dynamical quantities with evolution equations given by

$$\partial_t A_k + \partial_k [\alpha (f \text{tr} K - \lambda \Theta)] = 0 \quad (29)$$

$$\partial_t D_{kij} + \partial_k [\alpha K_{ij}] = 0 \quad (30)$$

(we will consider in what follows the vanishing shift case for simplicity), so that the full set of dynamical fields can be given by

$$u = \{\alpha, \gamma_{ij}, K_{ij}, A_k, D_{kij}, \Theta, Z_k\} \quad (31)$$

(38 independent fields).

Care must be taken when expressing the Ricci tensor ${}^{(3)}R_{ij}$ in (5) in terms of the derivatives of D_{kij} , because as far as the constraints (28) are no longer enforced, the identity

$$\partial_r D_{sij} = \partial_s D_{rij} \quad (32)$$

can not be taken for granted in first order systems. As a consequence of this ordering ambiguity of second derivatives, the principal part of the evolution equation (5) can

be written in a one-parameter family of non-equivalent ways, namely

$$\partial_t K_{ij} + \partial_k [\alpha \lambda_{ij}^k] = \dots \quad (33)$$

$$\begin{aligned} \lambda_{ij}^k &\equiv -\Gamma_{ij}^k + \frac{1-\zeta}{2} (D_{ij}^k + D_{ji}^k - \delta_i^k D_{rj}^r - \delta_j^k D_{ri}^r) \\ &+ \frac{1}{2} \delta_i^k (A_j + D_{jr}^r - 2Z_j) + \frac{1}{2} \delta_j^k (A_i + D_{ir}^r - 2Z_i) \end{aligned} \quad (34)$$

so that the parameter choice $\zeta = +1$ corresponds to the standard Ricci decomposition

$${}^{(3)}R_{ij} = \partial_k \Gamma_{ij}^k - \partial_i \Gamma_{kj}^k + \Gamma_{rk}^r \Gamma_{ij}^k - \Gamma_{ri}^k \Gamma_{kj}^r \quad (35)$$

whereas the opposite choice $\zeta = -1$ corresponds to the de Donder-Fock [31, 32] decomposition

$$\begin{aligned} {}^{(3)}R_{ij} &= -\partial_k D_{ij}^k + \partial_{(i} \Gamma_{j)k}^k - 2D_r^{rk} D_{kij} \\ &+ 4D^{rs}{}_i D_{rsj} - \Gamma_{irs} \Gamma_j^{rs} - \Gamma_{rij} \Gamma^{rk}{}_k \end{aligned} \quad (36)$$

which is most commonly used in Numerical Relativity codes. Note that this ambiguity does not affect to the principal part of eq. (6), namely

$$\partial_t \Theta + \partial_k [\alpha V^k] = \dots \quad (37)$$

where we have noted

$$V_k \equiv D_{kr}^r - D^r{}_{rk} - Z_k. \quad (38)$$

We are now in position to discuss the hyperbolicity of this first order version of the Z4 systems. This is done in a straightforward way in Appendix A.

In order to compare the new first order system with the Bona-Massó ones [9, 10] we could either apply here again the recombination (16) followed by the suppression (12) of the Θ field or we could take directly a first order version of the Z3 system (18-20). Eqs. (18,20,30) do not change, but eqs. (29,33,34) are replaced in this case by

$$\partial_t A_k + \partial_k [\alpha f \text{tr} K] = 0 \quad (39)$$

$$\partial_t K_{ij} + \partial_k [\alpha \lambda_{ij}^k] = \dots \quad (40)$$

$$\begin{aligned} \lambda_{ij}^k &\equiv -\Gamma_{ij}^k - \frac{n}{2} V^k \gamma_{ij} \\ &+ \frac{1}{2} \delta_i^k (A_j + D_{jr}^r - 2Z_j) + \frac{1}{2} \delta_j^k (A_i + D_{ir}^r - 2Z_i) \\ &+ \frac{1-\zeta}{2} (D_{ij}^k + D_{ji}^k - \delta_i^k D_{rj}^r - \delta_j^k D_{ri}^r) \end{aligned} \quad (41)$$

The full Bona-Massó family of evolution equations is recovered for the $\zeta = -1$ case, where (41) can be written as

$$\begin{aligned} \lambda_{ij}^k &\equiv D_{ij}^k - \frac{n}{2} V^k \gamma_{ij} \\ &+ \frac{1}{2} \delta_i^k (A_j - D_{jr}^r + 2V_j) + \frac{1}{2} \delta_j^k (A_i - D_{ir}^r + 2V_i) \end{aligned} \quad (42)$$

with V_k defined by (38).

In the following section, we will compare the behavior of both families in numerical simulations. To this end, we will also consider the first order version of the ADM system, which can be obtained from the previous ones just by suppressing the Z_i eigenfields.

$$Z_i = 0. \quad (43)$$

Before proceeding to the test section, let us just mention, that the same game of recombining the Θ field with K_{ij} (17) before suppressing it can also be played with the Z_k fields and D_{kij} in first order systems. As stated before, this will provide a complete symmetry breaking mechanism. We will do that in Appendix C, where we will show how the well known KST system [17] can also be recovered in that way from the Z4 framework discussed in this paper.

IV. TESTING SECOND AND FIRST ORDER SYSTEMS

We will present in this section a couple of numerical experiments which have been suggested very recently [30] as standard test-beds for Numerical Relativity codes. Our philosophy is that all the tests could be done “out of the box”, using well known numerical methods and the equations that are fully presented here: anyone should be able to reproduce our results without recourse to additional information.

We will use the standard method of lines [33] as a finite differencing algorithm, so that space and time discretization will be dealt separately. Space differencing will consist of taking centered discretizations of derivatives in our 3D grid. We use the standard centered stencil for first derivatives and we make sure that second derivatives, when needed, are coded also as centered derivatives of these first derivatives, even if it takes up to five point along every axis. In order to avoid boundary effects, the grid has the topology of a three-torus, with periodic boundaries along every axis. The time evolution will be dealt with a third order Runge-Kutta algorithm. The time step dt is kept small enough to avoid an excess of numerical dissipation that could distort our results in long runs.

A. Robust stability test

Let us consider a small perturbation of Minkowski space-time which is generated by taking random initial data for every dynamical field in the system. The level of the random noise must be small enough to make sure that we will keep in the linear regime even for a thousand of crossing times (the time that a light ray will take to cross the longest way along the numerical domain). This is in keeping with the theoretical framework of Appendix

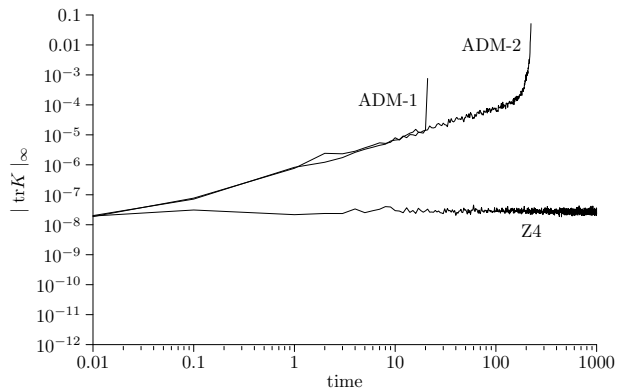


FIG. 1: The maximum of (the absolute value of) trK is plotted against the number of crossing times in a logarithmic scale. The initial level of random noise remains constant during the evolution in the case of strongly hyperbolic systems (only the second order Z4 system is shown here for clarity). In the case of weakly hyperbolic systems, like the ADM second order system ADM-2 or its first order version ADM-1, a linear growth is detected up to the point where the codes crash. Notice that the second order version is more robust, an order of magnitude, than the first one. The simulations are made with 50 grid points with $dt = 0.03 dx$.

A, where only linear perturbations around the Minkowski metric are considered.

We have plotted in Fig. 1 our results for the standard harmonic case (27). We see the expected polynomial (linear in this case) growth [27] of the weakly hyperbolic ADM system. Notice that modifications of the lower order terms (the ones not contributing to the principal part) could lead to catastrophic exponential growth, revealing an ill-posed evolution system [27]. In this paper, however, we will limit ourselves to discussing the linear regime as an hyperbolicity test for the principal part of the system. In this sense, the linear growth of the ADM plots in Fig. 1 confirms the weakly hyperbolic character of the ADM system.

The Z4 system shows instead the no-growth behavior, independent of the time resolution (see Figs. 1, 2), which one would expect from a strongly hyperbolic system. The same qualitative behavior is shown by the corresponding Z3 systems in (18-20), including the one with $n = 4/3$ that is quasiequivalent to the BSSN system.

We also show in Fig. 4 the same results, but distorted by using too much numerical dissipation: the time evolution here is dealt with the second order ICN method rather than the third order Runge-Kutta of Fig. 1. After hundreds of crossing times, the numerical dissipation manages to curve the linear growing of ADM and the noise level goes down in the Z4 case. This is just a numerical artifact, because in the linear regime there is no physical damping mechanism for strongly hyperbolic systems in a three-torus, where periodic boundary conditions do not allow propagation outside the domain. This

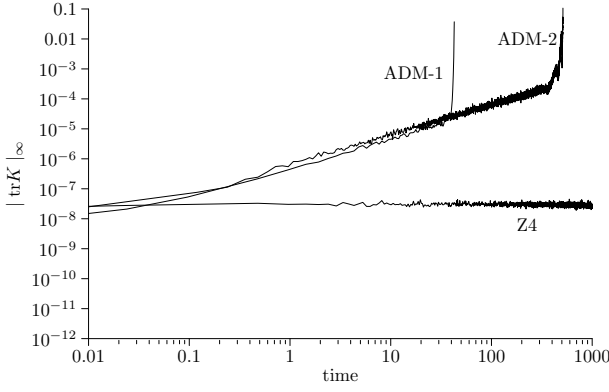


FIG. 2: Same as Fig. 1, but with less time resolution ($dt = 0.06 \, dx$ with the same dx). There is a slight amount of dissipation that delays the crashing of the ADM codes; this is especially visible for the second order version ADM-2, which keeps being more robust than its first order counterpart ADM-1. The behaviour of the Z4 code keeps unaffected.

is why we will use here third order Runge-Kutta instead of the ICN method proposed in [30].

In Fig. 3, we explore parameter space in the (f, λ) plane. If we interpret the constant behavior in Fig. 1 as revealing a strongly hyperbolic system and the polynomial growth (linear in this case) in Fig. 1 as revealing a weakly hyperbolic system, the results of our numerical experiment fully agree with the theoretical results pre-

FIG. 3: Array of results of numerical experiments in the gauge parameter plane (f, λ) , by using the Z4 system. A triangle stands for linear growth of noise (weak hyperbolicity), whereas a cross stands for a constant noise level (strong hyperbolicity). This is consistent with the strong hyperbolicity requirements predicted in Appendix B: either $f = 1$ and $\lambda = 2$, or $f \neq 1$ and $f > 0$.

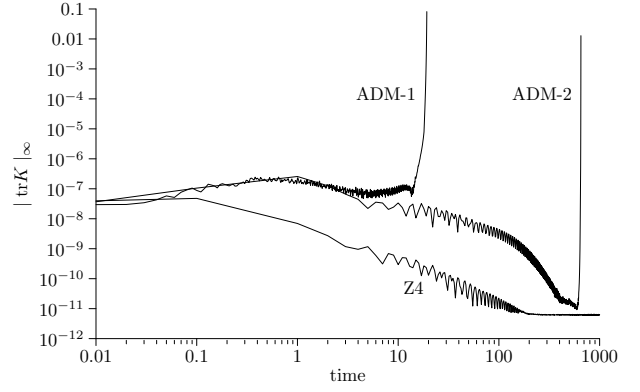
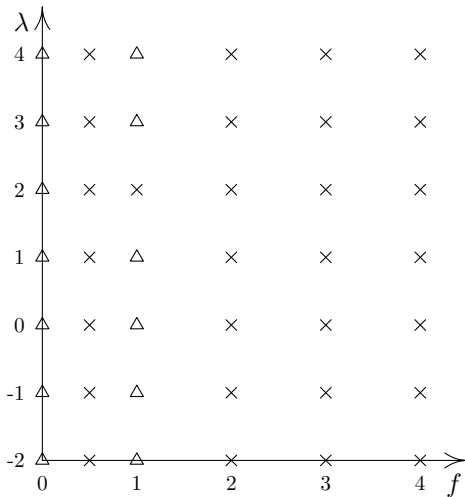


FIG. 4: Same as Fig. 1, but using the second order ICN method to evolve in time instead of a third order Runge-Kutta algorithm. Numerical dissipation is severely distorting the plots, by masking the linear growth in the weakly hyperbolic case and dramatically reducing the initial noise level in the strongly hyperbolic case. Notice that both dt and dx are the same as in Fig. 1 and we are using also the same space discretization algorithm: only the time evolution method has changed.

sented in Appendix A.

B. Gowdy waves

In order to test the strong field regime, let us consider now the Gowdy solution [34], which describes a space-time containing plane polarized gravitational waves (see also [35] for an excellent review of these space-times as cosmological models). The line element can be written as

$$ds^2 = t^{-1/2} e^{Q/2} (-dt^2 + dz^2) + t(e^P dx^2 + e^{-P} dy^2) \quad (44)$$

where the quantities Q and P are functions of t and z only and periodic in z , so that (44) is well suited for finite difference numerical grids with periodic boundary conditions along every axis. Following [30], we will choose the particular case

$$P = J_0(2\pi t) \cos(2\pi z) \quad (45)$$

$$Q = \pi J_0(2\pi) J_1(2\pi) - 2\pi t J_0(2\pi t) J_1(2\pi t) \cos^2(2\pi z) + 2\pi^2 t^2 [J_0^2(2\pi t) + J_1^2(2\pi t) - J_0^2(2\pi) - J_1^2(2\pi)] \quad (46)$$

so that it is clear that the lapse function

$$\alpha = t^{-1/4} e^{Q/4} \quad (47)$$

is constant everywhere at any time t_0 at which $J_0(2\pi t_0)$ vanishes. In [30] the initial slice $t = t_0$ was chosen for the simulation of the collapse, where $2\pi t_0$ is the 20-th root of the Bessel function J_0 , i.e. $t_0 \simeq 9.88$.

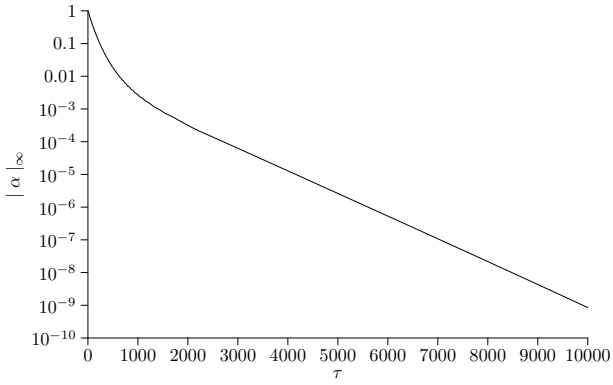


FIG. 5: Time evolution of (the maximum value of) the lapse function α in a collapsing Gowdy space-time (harmonic slicing). Notice that the harmonic time coordinate τ is not the proper time and it does not coincide with the number of crossing times, due to the collapse of the lapse, which is visible here, by a 10^{-9} factor.

Let us now perform the following time coordinate transformation

$$t = t_0 e^{-\tau/\tau_0}, \quad \tau_0 = t_0^{3/4} e^{Q(t_0)/4} \simeq 472, \quad (48)$$

so that the expanding line element (44) is seen in the new time coordinate τ as collapsing towards the $t = 0$ singularity, which is approached only in the limit $\tau \rightarrow \infty$. This “singularity avoidance” property of the τ coordinate is not surprising if one realizes that the resulting slicing by $\tau = \text{constant}$ surfaces is harmonic [36].

This means that we can launch our simulations starting with a constant lapse $\alpha_0 = 1$ at $\tau = 0$ ($t = t_0$) with the

FIG. 6: The quantity Θ is plotted as an indicator of the accumulated error of the simulations for the ADM, Z4 and Z3-BSSN second order forms. Even in this logarithmic scale, it can be clearly seen how the Z4 and Z3-BSSN codes perform much better than the ADM one: error differs by one order of magnitude at $\tau \simeq 1000$. The Z3-BSSN code gets closer to the Z4 one in the oscillatory phase (up to $\tau \simeq 2000$).

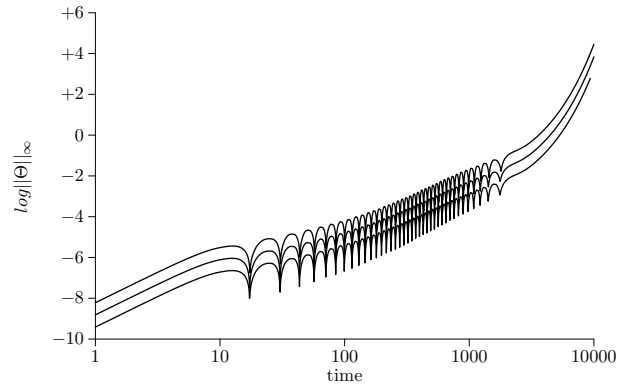
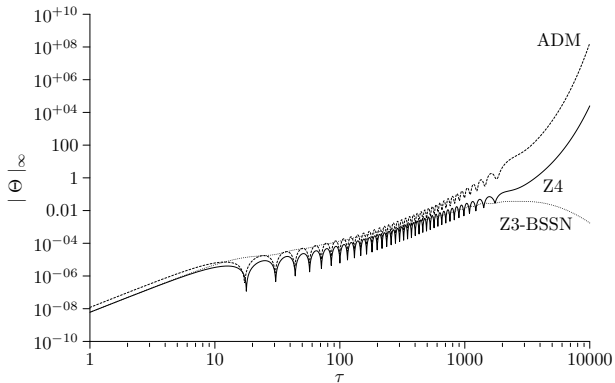
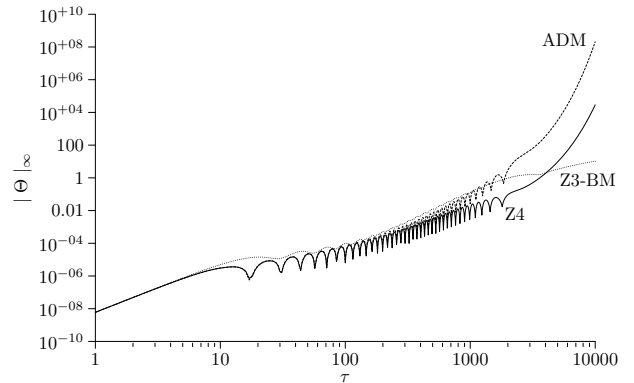


FIG. 7: Convergence test for the Z4 code. The three lines correspond to 50, 100 and 200 grid points. The quantity Θ itself is a direct measure of the error. In that logarithmic scale differences of $\log 4$ correspond to dividing by four the error when doubling the resolution. This second order convergence rate is clearly shown in the figure.

gauge parameter choice $f = 1$ (which means also $\lambda = 2$ in the Z4 case). Notice that the harmonic time coordinate τ is not the proper time and it does not coincide with the number of crossing times, due to the collapse of the lapse. Remember also that the local value of light speed (proper distance over coordinate time) is $\pm\alpha$. Even though in our plots τ goes up to 10000, the light ray manages to cross the domain in the z -direction only $t_0 \simeq 9.88$ times, as it follows from the original form (44) of the line element.

We plot in Fig. 5 the maximum values of the lapse function as time goes on, measured in terms of the harmonic time coordinate τ . Notice the huge magnitude of the dynamical space we are covering, as α goes down (col-

FIG. 8: Same as Fig. 6, but with the first order versions of both the ADM and Z4 codes, which behave in the same way as their second order counterparts. The Z3-BM code gets here closer the ADM one in the oscillatory phase (up to $\tau \simeq 2000$), in contrast with the behavior of the Z3-BSSN code in Fig. 6.

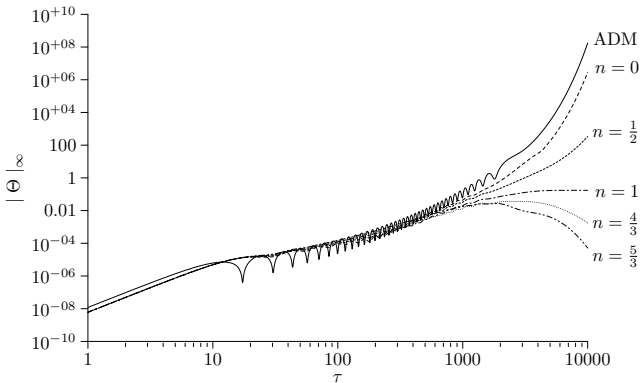


lapse of the lapse) by the factor of one billion during the simulation. This is a real challenge for numerical codes and all of them are doing quite well until $\tau = 1000$. The behavior at later times is dominated by the lower order terms: coordinate light speed ($\pm\alpha$) is so small that the dynamics of the principal part is frozen and care must be taken to avoid too big time steps. We have not seen any of the codes crashing even in very long simulations (up to $\tau = 60.000$) when the size of the time step is kept under control.

In Fig. 6, we use the quantity Θ , as computed from (6) to monitor the quality of the simulation both in the Z4 case (4-7), where Θ is a dynamical field, and in the other two second order cases (ADM and Z3-BSSN), where Θ is no longer a dynamical quantity but can still be used as a good measure of the error in the simulation. This makes easier to perform convergence tests (second order convergence is shown in Fig. 7). Notice that our Z3-BSSN code performs here much better than the original BSSN one [12], as reported in [30]. This is mainly due to the fact that we are not using here the conformal decomposition (22-24) which is at odds with the structure of the line element (44). This is why we talk here about Z3-BSSN (18-21) instead of simply BSSN.

The same kind of comparison is made in Fig. 8 for the first order version of the ADM and Z4 codes, which show the same behavior than their second order counterparts in Fig. 6. The third plot corresponds to the Z3 version of the Bona-Massó code, which can be obtained from (39-41), with the parameter choice $\zeta = -1$, $n = +1$. Notice that in the oscillatory phase (up to $\tau \simeq 2000$) the Z3-BM code tends to behave like the ADM one, whereas in Fig. 6 the Z3-BSSN code tends to behave more like the Z4 one.

FIG. 9: Same as Fig. 6, but with different values of the parameter n arising from the symmetry breaking mechanism in the Z3 codes. The differences show up in the collapse final phase (starting at $\tau \simeq 2000$). Notice that the value $n = 4/3$ corresponds to the Z3-BSSN case in Fig. 6, whereas the case $n = 1$ corresponds to (the second order version of) the Z3-BM case in Fig. 8. First order versions (not shown) behave in the same way as their second order counterparts shown here



Notice that the Z3 versions, when compared with both ADM and Z4, show a different behavior after the oscillatory phase: θ grows at a much lower rate or even starts going down. This behavior is due to the extra terms that appear in the evolution equations for K_{ij} after the symmetry breaking, which can be controlled by the parameter n introduced in (17). This point is clearly shown in Fig. 9, where different choices of n produce different behavior in the final collapse phase (starting at $\tau \simeq 2000$). This shows the relevance of the recombination between the dynamical fields in numerical applications, as pointed out in [17]. Further details and other numerical tests can be found in the webpage at <http://stat.uib.es>.

Appendix A: Hyperbolicity of the Second Order Z4 System

Let us consider the linearized version of the Z4 system (4-7) around Minkowski space-time in order to study the propagation of a plane wave in that background:

$$\gamma_{ij} = \delta_{ij} + 2 e^{i \omega \cdot x} \hat{\gamma}_{ij}(\omega, t) \quad (\text{A.1})$$

$$\alpha = 1 + e^{i \omega \cdot x} \hat{\alpha}(\omega, t) \quad (\text{A.2})$$

$$K_{ij} = i \omega e^{i \omega \cdot x} \hat{K}_{ij}(\omega, t) \quad (\text{A.3})$$

$$\Theta = i \omega e^{i \omega \cdot x} \hat{\Theta}(\omega, t) \quad (\text{A.4})$$

$$Z_k = i \omega e^{i \omega \cdot x} \hat{Z}_k(\omega, t) \quad (\text{A.5})$$

where we will take for simplicity $\beta^i = 0$ and

$$\omega_k = \omega n_k, \quad \delta^{ij} n_i n_j = 1 \quad (\text{A.6})$$

The Z4 system reads then

$$\partial_t \hat{\gamma}_{ij} = -i \omega \hat{K}_{ij} \quad (\text{A.7})$$

$$\partial_t \hat{\alpha} = -i \omega [f \text{tr} \hat{K} - \lambda \hat{\Theta}] \quad (\text{A.8})$$

$$\partial_t \hat{\Theta} = -i \omega [\text{tr} \hat{\gamma} - \hat{\gamma}^{nn} - \hat{Z}^n] \quad (\text{A.9})$$

$$\partial_t \hat{Z}_k = -i \omega [n_k (\text{tr} \hat{K} - \hat{\Theta}) - \hat{K}_k^n] \quad (\text{A.10})$$

$$\partial_t \hat{K}_{ij} = -i \omega \hat{\lambda}_{ij} \quad (\text{A.11})$$

where we have noted

$$\begin{aligned} \hat{\lambda}_{ij} \equiv & \hat{\gamma}_{ij} + n_i n_j (\hat{\alpha} + \text{tr} \hat{\gamma}) \\ & - n_i (\hat{\gamma}_j^n + \hat{Z}_j) - n_j (\hat{\gamma}_i^n + \hat{Z}_i) \end{aligned} \quad (\text{A.12})$$

and where the symbol n replacing an index means the contraction with n_i . It can be also expressed in matrix form, namely

$$\hat{u} = (\hat{\alpha}, \hat{\gamma}_{ij}, \hat{K}_{ij}, \hat{\Theta}, \hat{Z}_k) \quad (\text{A.13})$$

$$\partial_t \hat{u} = -i \omega \mathbf{A} \hat{u} \quad (\text{A.14})$$

The spectral analysis of the characteristic matrix \mathbf{A} provides the following list of eigenvalues and eigenfields

a) Standing eigenfields (zero characteristic speed)

$$\hat{\alpha} - f \text{tr} \hat{\gamma} + \lambda (\text{tr} \hat{\gamma} - \hat{\gamma}^{nn} - \hat{Z}^n), \quad \hat{\gamma}_\perp^n + \hat{Z}_\perp \quad (\text{A.15})$$

where the symbol \perp replacing an index means the projection orthogonal to n_i .

b) Light-cone eigenfields (characteristic speed ± 1)

$$\hat{K}_{\perp\perp} \pm \hat{\gamma}_{\perp\perp} \quad (\text{A.16})$$

$$\hat{K}_\perp^n \pm \hat{Z}_\perp \quad (\text{A.17})$$

$$\hat{\Theta} \pm [\text{tr} \hat{\gamma} - \hat{\gamma}^{nn} - \hat{Z}^n]. \quad (\text{A.18})$$

Notice that (A.16-A.18) can be seen as the components of a tensor:

$$\begin{aligned} \hat{L}_{ij}^\pm &\equiv [\hat{K}_{ij} - (\text{tr} \hat{K} - 2\hat{\Theta}) n_i n_j] \\ &\pm [\hat{\lambda}_{ij} - \hat{\alpha} n_i n_j] \end{aligned} \quad (\text{A.19})$$

c) Gauge eigenfields (characteristic speed $\pm \sqrt{f}$)

$$\begin{aligned} \hat{G}^\pm &\equiv \sqrt{f} \left[\text{tr} \hat{K} + \frac{2-\lambda}{f-1} \hat{\Theta} \right] \\ &\pm \left[\hat{\alpha} + \frac{2f-\lambda}{f-1} (\text{tr} \hat{\gamma} - \hat{\gamma}^{nn} - \hat{Z}^n) \right] \end{aligned} \quad (\text{A.20})$$

From (A.15-A.20) we can easily conclude [26, 27]

- i) All the characteristic speeds are real (weak hyperbolicity at least) if and only if $f \geq 0$.
- ii) In the case $f = 0$, the two components of the gauge pair (A.20) are not independent, so that the total number of independent eigenfields is 16 instead of 17 required for strong hyperbolicity.
- iii) The case $f = 1$ (harmonic case) is special:
 - if $\lambda \neq 2$, then the gauge pair (A.20), which can be previously rescaled by a $(f-1)$ factor, is equivalent to (A.18), so that one has only 15 independent eigenfields
 - if $\lambda = 2$, then the quotient $\frac{2-\lambda}{f-1}$ can take any value, reflecting the degeneracy of the gauge and light cone eigenfields. One can then recover the full set of 17 independent eigenfields (strong hyperbolicity).
- iv) In all the remaining cases ($f > 0$, $f \neq 1$), the system is strongly hyperbolic, as we can recover the full set of 17 independent eigenfields.

Appendix B: Hyperbolicity of the First Order Z4 System

The principal part of the first order Z4 evolution system (4-7, 26, 29-30) can be written as (vanishing shift

case):

$$\partial_t \gamma_{ij} = \dots, \quad \partial_t \alpha = \dots \quad (\text{B.1})$$

$$\partial_t \Theta + \partial_k [\alpha V^k] = \dots \quad (\text{B.2})$$

$$\partial_t Z_i + \partial_k [\alpha (\delta_i^k (\text{tr} K - \Theta) - K^k_i)] = \dots \quad (\text{B.3})$$

$$\partial_t A_k + \partial_k [\alpha (f \text{tr} K - \lambda \Theta)] = \dots \quad (\text{B.4})$$

$$\partial_t D_{kij} + \partial_k [\alpha K_{ij}] = \dots \quad (\text{B.5})$$

$$\partial_t K_{ij} + \partial_k [\alpha \lambda_{ij}^k] = \dots \quad (\text{B.6})$$

where

$$\begin{aligned} \lambda_{ij}^k &= D^k_{ij} - \frac{1+\zeta}{2} (D_{ij}^k + D_{ji}^k - \delta_i^k D_{rj}^r - \delta_j^k D_{ri}^r) \\ &+ \frac{1}{2} \delta_i^k (A_j - D_{jr}^r + 2V_j) \\ &+ \frac{1}{2} \delta_j^k (A_i - D_{ir}^r + 2V_i) \end{aligned} \quad (\text{B.7})$$

$$V_k \equiv D_{kr}^r - D_{rk}^r - Z_k. \quad (\text{B.8})$$

Now, if we consider the propagation of perturbations with wavefront surfaces given by the unit (normal) vector n_i , we can express (B.1-B.6) in matrix form

$$\alpha^{-1} \partial_t u + \mathbf{A}(u) n^k \partial_k u = \dots, \quad (\text{B.9})$$

where

$$u = \{\alpha, \gamma_{ij}, K_{ij}, A_k, D_{kij}, \Theta, Z_k\}. \quad (\text{B.10})$$

(notice that derivatives tangent to the wavefront surface play no role here).

A straightforward analysis of the characteristic matrix $\mathbf{A}(u)$ provides the following list of eigenfields:

a) Standing eigenfields (zero characteristic speed)

$$\alpha, \gamma_{ij}, A_\perp, D_{\perp ij}, A_k - f D_k + \lambda V_k \quad (\text{B.11})$$

(24 independent fields), where the symbol \perp replacing an index means the projection orthogonal to n_i :

$$D_{\perp ij} \equiv D_{kij} - n_k n^r D_{rij}. \quad (\text{B.12})$$

b) Light-cone eigenfields (characteristic speed ± 1)

$$\begin{aligned} L_{ij}^\pm &\equiv [K_{ij} - n_i n_j \text{tr} K] \\ &\pm [\lambda_{ij}^n - n_i n_j \text{tr} \lambda^n] \end{aligned} \quad (\text{B.13})$$

$$L^\pm \equiv \theta \pm V^n \quad (\text{B.14})$$

(12 independent fields), where the symbol n replacing the index means the contraction with n_i

$$\lambda_{ij}^n \equiv n_k \lambda_{ij}^k. \quad (\text{B.15})$$

c) Gauge eigenfields (characteristic speed $\pm \sqrt{f}$)

$$\begin{aligned} G^\pm &\equiv \sqrt{f} \left[\text{tr} K + \frac{2-\lambda}{f-1} \Theta \right] \\ &\pm \left[A^n + \frac{2f-\lambda}{f-1} V^n \right] \end{aligned} \quad (\text{B.16})$$

From (B.11-B.16) we can easily conclude that

- i) All the characteristic speeds are real (weak hyperbolicity at least) if and only if $f \geq 0$.
- ii) In the case $f = 0$, the two components of the pair (B.16) are not independent, so that the total number of independent eigenfields is 37 instead of 38 required for strong hyperbolicity.
- iii) The case $f=1$ (harmonic case) is special:
 - if $\lambda \neq 2$, then the pair of fields (B.16) is the same as (B.14), so that one has only 36 independent eigenfields
 - if $\lambda = 2$, then the quotient $\frac{2-\lambda}{f-1}$ can take any value due to the degeneracy of the gauge and light eigenfields. One can then recover the full set of 38 independent eigenfields (strong hyperbolicity).
- iv) The first order Z4 system described by (B.1-B.6) is strongly hyperbolic in all the remaining cases ($f > 0, f \neq 1$).

Notice also that the special (harmonic) case $f = 1, \lambda = 2$ has been shown in [25] to be symmetric hyperbolic for the parameter choice $\zeta = -1$. The corresponding energy function can be written as

$$E \equiv K^{ij} K_{ij} + \lambda^{kij} \lambda_{kij} + (\text{tr} K - 2\Theta)^2 + A^k A_k + (A^k - D^{kr}{}_r + 2V^k)(A_k - D_{kr}{}^r + 2V_k) \quad (\text{B.17})$$

but notice that this expression is far from being unique. For instance, allowing for (B.11), the last term in (B.17) could appear with any arbitrary factor.

Appendix C: Recovering the KST systems

Let us start with the first order Z4 evolution system (4-7,26,29-30) where the principal part is given by (B.1-B.8). Now let us follow the two step ‘symmetry breaking’ process, namely

- i) Recombine the dynamical fields K_{ij}, D_{kij} with Θ and Z_i in a linear way,

$$\tilde{K}_{ij} = K_{ij} - \frac{n}{2} \Theta \gamma_{ij}, \quad (\text{C.1})$$

$$d_{kij} = 2D_{kij} + \eta \gamma_{k(i} Z_{j)} + \chi Z_k \gamma_{ij}, \quad (\text{C.2})$$

where we have used the notation of Ref. [17], replacing only their parameter γ by $-n/2$ for consistency. Notice that (C.1-C.2) is generic in the sense that it is the most general linear combination that preserves the tensor character of the dynamical fields under linear coordinate transformations.

- ii) Suppress both θ and Z_i as dynamical fields, namely

$$\Theta = 0, \quad Z_i = 0. \quad (\text{C.3})$$

In that way, the principal part (B.1-B.8) becomes

$$\partial_t \gamma_{ij} = \dots, \quad \partial_t \alpha = \dots \quad (\text{C.4})$$

$$\partial_t A_k + \partial_k [\alpha f \text{tr} \tilde{K}] = 0 \quad (\text{C.5})$$

$$\begin{aligned} \partial_t d_{kij} + \partial_r [\alpha \{ 2 \delta_k^r \tilde{K}_{ij} - \chi (\tilde{K}_k^r - \delta_k^r \text{tr} \tilde{K}) \gamma_{ij} \\ + \eta \gamma_{k(i} (\tilde{K}^r{}_{j)} - \delta^r{}_{j)} \text{tr} \tilde{K}) \}] = \dots \end{aligned} \quad (\text{C.6})$$

$$\partial_t \tilde{K}_{ij} + \partial_k [\alpha \lambda_{ij}^k] = \dots \quad (\text{C.7})$$

$$\begin{aligned} 2 \lambda^k{}_{ij} = d^k{}_{ij} - \frac{n}{4} (d_{kr}{}^r - d_r{}^{rk}) \gamma_{ij} \\ + \frac{1+\zeta}{2} (d_{ij}{}^k + d_{ji}{}^k) - \frac{1-\zeta}{2} (\delta_i^k d_{rj}{}^r + \delta_j^k d_{ri}{}^r) \\ + \delta_j^k (A_i + \frac{1}{2} d_{ir}{}^r) + \delta_i^k (A_j + \frac{1}{2} d_{jr}{}^r) \end{aligned} \quad (\text{C.8})$$

for the reduced set of variables

$$u = \{ \alpha, \gamma_{ij}, \tilde{K}_{ij}, A_k, d_{kij} \}. \quad (\text{C.9})$$

This provides a “dynamical lapse” version [18] of the KST evolution systems. In order to recover the original “densitized lapse” version, one must in addition integrate explicitly the dynamical relationship (26) between the lapse and the volume element (remember that now $\Theta = 0$). It can be easily done in the case

$$f = 2\sigma = \text{constant}, \quad (\text{C.10})$$

namely

$$\partial_t (\alpha \gamma^{-\sigma}) = 0, \quad (\text{C.11})$$

so that the value of α can be defined in terms of γ for every initial condition. The same thing can be done with A_i and d_i , so that

$$A_i \equiv \sigma d_{ir}{}^r + \dots \quad (\text{C.12})$$

and the set of dynamical fields is then further reduced to

$$u = \{ \gamma_{ij}, K_{ij}, d_{kij} \}. \quad (\text{C.13})$$

The principal part of the evolution system is then given by (we suppress the tildes over the K_{ij})

$$\partial_t \gamma_{ij} = \dots \quad (\text{C.14})$$

$$\begin{aligned} \partial_t d_{kij} + \partial_r [\alpha \{ 2 \delta_k^r K_{ij} - \chi (K_k^r - \delta_k^r \text{tr} K) \gamma_{ij} \\ + \eta \gamma_{k(i} (K^r{}_{j)} - \delta^r{}_{j)} \text{tr} K) \}] = \dots \end{aligned} \quad (\text{C.15})$$

$$\partial_t K_{ij} + \partial_k [\alpha \lambda_{ij}^k] = \dots \quad (\text{C.16})$$

$$\begin{aligned}
2 \lambda^k_{ij} &= d^k_{ij} - \frac{n}{4}(d_{kr}{}^r - d_r{}^{rk})\gamma_{ij} \\
&- \frac{1-\zeta}{2}(\delta_i^k d^r{}_{rj} + \delta_j^k d^r{}_{ri}) + \frac{1+\zeta}{2}(d_{ij}{}^k + d_{ji}{}^k) \\
&+ \frac{1+2\sigma}{2}(\delta_i^k d_{jr}{}^r + \delta_j^k d_{ir}{}^r) \quad (C.17)
\end{aligned}$$

which corresponds precisely to (the principal part of) the original KST system [17].

Acknowledgements: This work has been supported by the EU Programme 'Improving the Human Research Potential and the Socio-Economic Knowledge Base' (Research Training Network Contract HPRN-CT-2000-00137), by the Spanish Ministerio de Ciencia y Tecnología through the research grant number BFM2001-0988 and by a grant from the Conselleria d'Innovació i Energia of the Govern de les Illes Balears.

-
- [1] <http://www.ligo.caltech.edu>.
 - [2] <http://www.virgo.infn.it>.
 - [3] <http://www.geo600.uni-hannover.de>.
 - [4] <http://tamago.mtk.nao.ac.jp>.
 - [5] S. Brandt et al, Phys. Rev. Lett. **85** 5496 (2000).
 - [6] R. Arnowit, S. Deser and C. W. Misner, *Gravitation: an introduction to current research*, ed. L. Witten, Wiley, New York (1962).
 - [7] J. Centrella, Phys. Rev. D **21**, 2776 (1980).
 - [8] Y. Choquet-Bruhat and T. Ruggeri, Comm. Math. Phys. **89**, 269 (1983).
 - [9] C. Bona and J. Massó, Phys. Rev. Lett. **68** 1097 (1992).
 - [10] C. Bona, J. Massó, E. Seidel and J. Stela, Phys. Rev. Lett. **75** 600 (1995).
 - [11] M. Shibata and T. Nakamura, Phys. Rev. D **52** 5428 (1995).
 - [12] T. W. Baumgarte and S. L. Shapiro, Phys. Rev. D **59** 024007 (1999).
 - [13] S. Frittelli and O. A. Reula, Commun. Math. Phys. **166** 221 (1994).
 - [14] S. Frittelli and O. A. Reula, Phys. Rev. Lett. **76** 4667 (1996).
 - [15] A. Anderson and J. W. York, Jr., Phys. Rev. Lett. **82** 4384 (1999).
 - [16] S. D. Hern, Ph. D. Thesis, gr-qc/0004036.
 - [17] L. E. Kidder, M. A. Scheel and S. A. Teukolsky, Phys. Rev. D **64**, 064017 (2001).
 - [18] O. Sarbach and M. Tiglio, Phys. Rev. D **66**, 064023 (2002).
 - [19] A. Abrahams, A. Anderson, Y. Choquet-Bruhat and J. W. York, Phys. Rev. Lett. **75**, 3377 (1995).
 - [20] H. Friedrich, Class. Quantum. Grav. **13**, 1451 (1996).
 - [21] O. Brodbeck, S. Frittelli, P. Hubner and O. Reula, J. Math. Phys. **40**, 909-923 (1999).
 - [22] H. Shinkai and G. Yoneda, "Progress in Astronomy and Astrophysics" (Nova Science Publ), to be published. Also available in gr-qc/0209111
 - [23] C. Bona et al, in preparation.
 - [24] A. P. Gentle, N. D. George, A. Kheyfets and W. A. Miller, gr-qc/0307007.
 - [25] C. Bona, T. Ledvinka, C. Palenzuela, M. Žáček, Phys. Rev. D **67**, 104005 (2003).
 - [26] H. O. Kreiss and O. E. Ortiz, Lect. Notes Phys. **604** (2002) 359.
 - [27] H. O. Kreiss and J. Lorentz, "Initial-Boundary Value Problems and the Navier-Stokes Equations" in Pure and Applied Mathematics, Vol. 136 (Academic Press Inc., San Diego 1989).
 - [28] O. Reula, Talk at the Hyperbolic Models for Astrophysics and Cosmology Workshop (submitted to Phys. Rev. D)
 - [29] C. Bona, T. Ledvinka and C. Palenzuela, Phys. Rev. D **66**, 084013 (2002).
 - [30] M. Alcubierre et al, gr-qc/0305023.
 - [31] T. De Donder, *La Gravifique Einsteinienne* Gauthier-Villars, Paris (1921).
 - [32] Fock, V.A., *The theory of Space Time and Gravitation*, Pergamon, London (1959).
 - [33] O. A. Liskovets, Differential equations I 1308-1323 (1965).
 - [34] R. H. Gowdy, Phys. Rev. D **27**, 826 (1971).
 - [35] B. Berger, submitted to Phys. Rev. D (2002), gr-qc/0207035.
 - [36] C. Bona and J. Massó, Phys. Rev. D **38** 2419 (1988).